Advances in Engineering Research : Possibilities and Challenges
ISSN Print: 3079-5192
ISSN Online: 3079-5206
https://doi.org/10.63313/AERpc.9045

Wear Prediction for Helical Gears Used in EMU

Delong Shao. Hanjun Jiang and Hao Wu
College of Mechanical and Automotive Engineering, Qingdao University of Technology, Qingdao, China
Email: sdl1612023@163.com

How to cite this paper: Shao, D. L., Jiang, H. J., & Wu, H. (2025). Wear Prediction for Helical Gears Used in EMU. *Advances in Engineering Research : Possibilities and Challenges*, 2(2), 18-25. ISSN Print: 3079-5192; ISSN Online: 3079-5206.
https://doi.org/10.63313/AERpc.9045
Published: 2025-08-15

Abstract

By combining Hertz contact theory with the Archard wear formula, a wear model for the tooth surface of helical cylindrical gears used in high-speed trains was developed, and its wear characteristics were numerically simulate.The simulation findings show that, under ideal operating conditions, the tooth sur-face of the helical gear pair wears non-uniformly along the tooth width direc-tion, with the least wear near the pitch circle and the most wear at the root of the smaller gear. Based on this, the effects of various modules, tooth width, he-lix angle, and input torque on tooth surface wear are investigated further. The analysis shows that changes in module, input torque, and tooth width all have a considerable impact on the distribution of tooth surface wear, although varia-tions in helix angle have a modest impact.

Keywords

Dry friction; Helical gear; Adhesion wear; Meshing characteristic

1. Introduction

Gears, as core components of various power transmission devices, are widely used in fields such as coal mine machinery, aerospace, and rail transit.The tooth surface wear behavior has a significant impact on the service life of the transmission system. A large number of studies have been carried out on gear wear issues. A few scholars have established different wear models using various methods [1-3], but the Archard wear model remains the most widely used one.Flodin et al. [4-5] established tooth surface wear models for spur and helical gears based on the simplified Winkler model and Archard wear formula, and numerically simulated the wear amount along the tooth profile direction. Bajpai et al. [6-7] developed a wear model for helical gear pairs based on three-dimensional finite element contact analysis. Hegadekatte et al. [8] calculated the wear of micro silicon nitride planetary gear trains using the finite element contact model and Archard wear formula. In addition, Ding and Liu introduced the dynamic wear coefficient into the wear calculation of spur gears and studied the coupling effect between tooth surface wear and system dynamic response [9,10]. The results showed that while tooth surface wear significantly changes the amplitude and frequency of the system, dynamic working conditions also significantly affect the amount and distribution of tooth surface wear. Osman proposed a slight wear calculation model for wide-tooth spur gears and helical gears, and comparatively analyzed the gear wear characteristics under quasi-static and dynamic loads [11].In this paper, taking involute helical gear transmission as the research object, according to its meshing characteristics,it is equivalent to a pair of reverse tapered roller contacts. A calculation model for tooth surface adhesive wear of helical gear transmission under dry friction condition is established based on the classical Archard wear formula. The distribution law of cumulative wear depth on the tooth surfaces of driving and driven gears under given working conditions is studied, and the influences of different tooth profile parameters on the tooth surface wear depth and distribution law are discussed.

2. Research on the meshing characteristics of helical gears

Based on the relationship between the transverse contact ratio εα and the axial contact ratio εβ, the variation of the contact line length on the meshing plane can be divided into two cases, as shown in Figure 1.

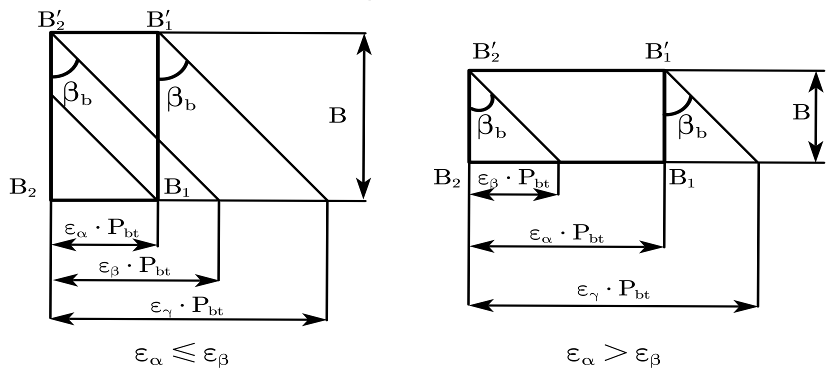

Figure 1. The length of the contact line on the meshing plane of involute helical gear transmission

In the case of the left diagram in Figure 1, the contact line length of the helical gear transmission can be expressed as

$$l(1,t)=\begin{cases} \dfrac{p_{bt}}{\sin\beta_b}\cdot\dfrac{t}{T_m} & 0\le t\le \varepsilon_\alpha\cdot T_m \\ \dfrac{p_{bt}}{\sin\beta_b}\cdot\varepsilon_\alpha & \varepsilon_\alpha\cdot T_m < t\le \varepsilon_\beta\cdot T_m \\ \dfrac{p_{bt}}{\sin\beta_b}\left(\varepsilon_\gamma-\dfrac{t}{T_m}\right) & \varepsilon_\beta\cdot T_m < t\le\varepsilon_\gamma\cdot T_m \\ 0 & \varepsilon_\gamma\cdot T_m < t\le ceil(\varepsilon_\gamma)\cdot T_m \end{cases} \tag{1}$$

In the case of the right diagram in Figure 1, the contact line length of the helical gear transmission can be expressed as

$$l(1,t)=\begin{cases}\dfrac{p_{bt}}{\sin\beta_b}\cdot\dfrac{t}{T_m} & 0\le t\le\varepsilon_\beta\cdot T_m\\ \dfrac{p_{bt}}{\sin\beta_b}\cdot\varepsilon_\alpha & \varepsilon_\beta\cdot T_m<t\le\varepsilon_\alpha\cdot T_m\\ \dfrac{p_{bt}}{\sin\beta_b}\left(\varepsilon_\gamma-\dfrac{t}{T_m}\right) & \varepsilon_\alpha\cdot T_m<t\le\varepsilon_\gamma\cdot T_m\\ 0 & \varepsilon_\gamma\cdot T_m<t\le ceil(\varepsilon_\gamma)\cdot T_m\end{cases} \tag{2}$$

In the formula, Tm represents the meshing period, pbt represents the end face pitch. According to the periodicity of meshing, the length of the nth contact line at time t can be expressed as

$$l(n,t)=l[1,t+(n-1)T_m] \tag{3}$$

The total contact line length at any moment can be expressed as

$$L(t)=l(1,t)+l(2,t)+\cdots+l(M,t)=\sum_{n=1}^{N}l(i,t) \tag{4}$$

Based on the difference in the percentage of each contact line length to the total contact line length at each moment, the quasi-static load on the tooth surface borne by the first pair of meshing teeth can be expressed as

$$F(1,t)=F_n\cdot\frac{l(1,t)}{L(t)} \tag{5}$$

In gear contact analysis, spur gear pairs are usually equivalent to a pair of disks with continuously changing radii, while helical gears are regarded as multiple spur gear slices stacked along the axis and rotated by a small angle in sequence, as shown in Figure 2.

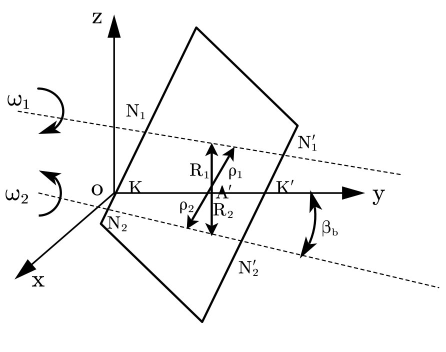

Figure 2. Equivalent Model of Single-Pair Teeth for Involute Helical Gears

On any given contact line, take an arbitrary point A(i, j). The radii of curvature of the driving wheel (denoted as R_1), the driven wheel (denoted as R_2), and the radius of curvature (denoted as R) at this point can be expressed as

$$\begin{cases} R_1(i,j) = [N_1B_2 + (i-1)L/i]/\cos\beta_b \\ R_2(i,j) = \{N_1N_2 - [N_1B_2 + (i-1)L/i]\}/\cos\beta_b \\ R(i,j) = R_1(i,j)R_2(i,j)/R_1(i,j) + R_2(i,j) \end{cases} \tag{6}$$

N_1N_2 represents the theoretical meshing line length.

The tangential velocity, relative sliding velocity u_s, entraining velocity u_r, and slide-roll ratio S_r of the two gears at the meshing point A can be expressed as

$$\begin{cases} u_1 = \omega_1 R_1(i,j)\cos\beta_b \\ u_2 = \omega_2 R_2(i,j)\cos\beta_b \end{cases} \tag{7}$$

$$\begin{cases} u_s(i,j) = |u_1(i,j) - u_2(i,j)| \\ u_r(i,j) = [u_1(i,j) - u_1(i,j)]/2 \\ S_r(i,j) = u_s(i,j)/u_r(i,j) \end{cases} \tag{8}$$

The slip distances at a meshing point on the tooth profiles of the driving wheel and the driven wheel are respectively expressed as

$$\begin{cases} S_1(i,j) = 2b|u_1(i,j) - u_2(i,j)|/u_1(i,j) \\ S_2(i,j) = 2b|u_1(i,j) - u_2(i,j)|/u_2(i,j) \end{cases} \tag{9}$$

The contact half-width at the meshing point

$$b = \sqrt{4wR/\pi E'} \tag{10}$$

E 'is the comprehensive radius of curvature

3. Calculation of adhesive wear on helical gear tooth surfaces

The calculation of adhesive wear for helical gears is typically based on the Archard wear model, and the wear volume under dry friction conditions.

$$V_{dry} = K\frac{FS}{H} \tag{11}$$

In the formula, K is the dimensionless wear coefficient of the gear material, and S is the relative sliding distance.

Average contact pressure at the meshing position.

$$p(i,j)=\frac{4F(1,t)}{3\pi bl(1,t)} \tag{12}$$

Thus, the tooth surface wear depth of the driving wheel and the driven wheel at a certain meshing position after one meshing cycle under dry contact conditions is obtained as

$$h_{dry1,2}(i,j)=kp(i,j)S_{1,2}(i,j) \tag{13}$$

After N meshing cycles, the accumulated wear depth of the tooth surface.

$$h_{x1,2}(i,j)=\sum_{n=1} h_{dry1,2}(i,j) \tag{14}$$

4. Results and Discussion

The geometric parameters of gears in the transmission system for EMUs (Electric Multiple Units) are shown in Table 1.

Table 1. Gear geometric parameters

Tooth number Z pinion	35
Tooth number Z gear	85
Tooth width B(mm)	65
Pressure angle α(°)	20
Addendum coefficient h_a	1
Tip clearance coefficient c	0.25
Module m(mm)	6
helical angle (°)	10

The figure shows the time-varying contact line length and time-varying load per unit contact line of the helical gear. It can be seen from the right part of Figure 3 that during the meshing process, both the length of a single contact line l(1,t) and the total length of multiple contact lines L(t) change continuously with meshing time: in the meshing-in process, l(1,t) increases continuously; in the middle meshing area, its value remains constant; in the meshing-out process, its value gradually decreases to zero. l(1,t) transitions continuously, while L(t) shows periodic changes. This meshing characteristic of helical gears ensures the continuous change of load, and the variation trend of the load per unit contact line is exactly opposite to that of L(t), as shown in the left part of Figure 3.

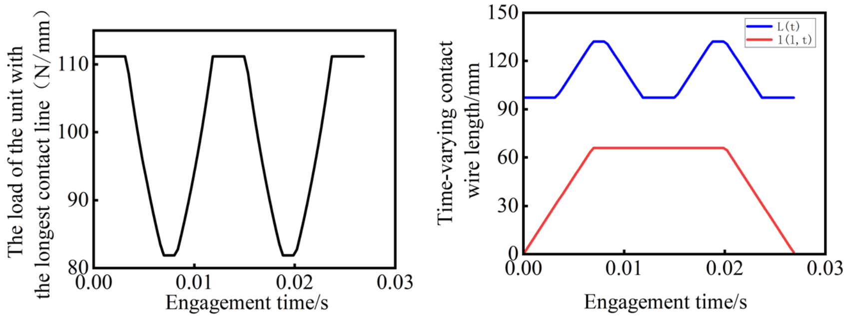

Figure 3. Time-varying contact line length and time-varying load per unit contact line

Figure 4 shows the tooth surface wear amounts of the driving and driven wheels after 1×10^5 load cycles. It can be seen from the figure that: the maximum wear amount of the driving wheel in the left figure is larger than that of the driven wheel in the right figure; the wear amounts at the tooth root and tooth tip of both the driving and driven gears are relatively large, and the wear amount at the tooth root is greater than that at the tooth tip, while the wear amount at the pitch circle tends to zero; the wear amount is non-uniformly distributed along the tooth width direction, and the wear amount of the driving wheel decreases sequentially from the front end face to the rear end face, whereas that of the driven wheel increases sequentially from the front end face to the rear end face.

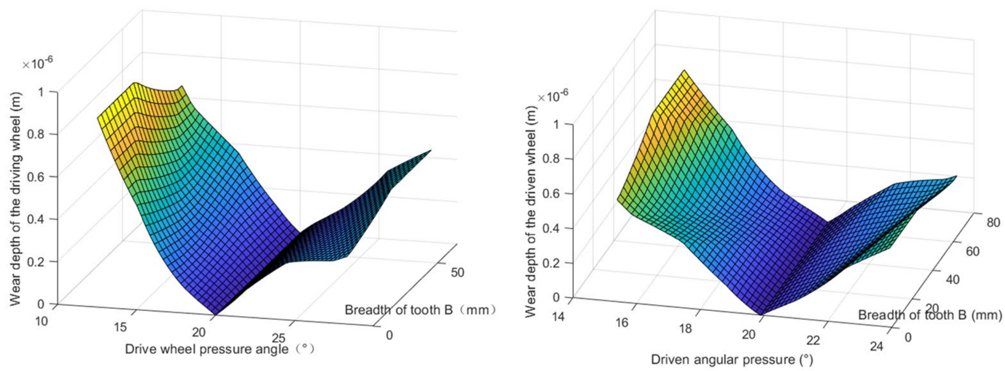

Figure 4. The wear depth of the driving and driven wheels

Figure 5 shows the tooth surface wear amounts of the driving wheel when the modules are 4mm, 5mm, and 6mm respectively. As the module increases, the tooth surface wear amount decreases, among which the wear amount from the pitch point to the tooth root segment drops sharply.

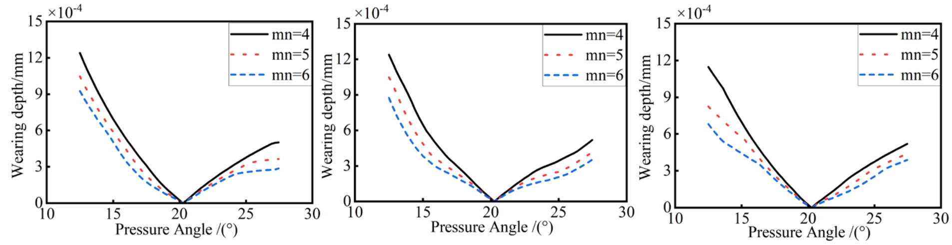

Figure 5. Comparison of the wear depth of the front, middle and rear end faces under different modules

Figure 6 shows the tooth surface wear amounts of the driving wheel under the input torques of 600 N·m, 800 N·m, and 1000 N·m, respectively. It can be seen from the figure that as the input torque increases, the tooth surface wear amount increases significantly.

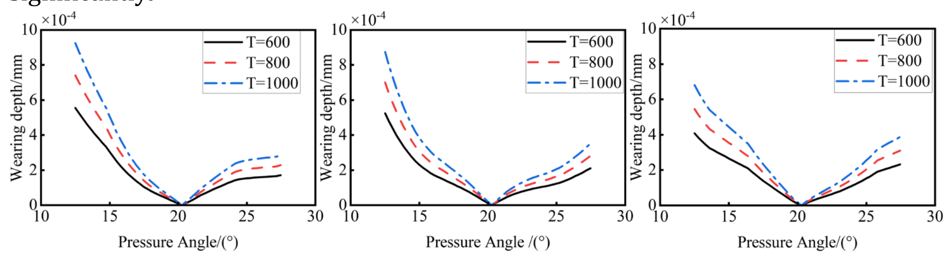

Figure 6. The wear amounts of the front, middle and rear end faces under different torques

Figure 7 shows the tooth surface wear amounts of the driving wheel when the helix angles are 10°, 14°, and 18° respectively. It can be seen from the figure that as the helix angle increases, the tooth surface wear amount decreases slightly.

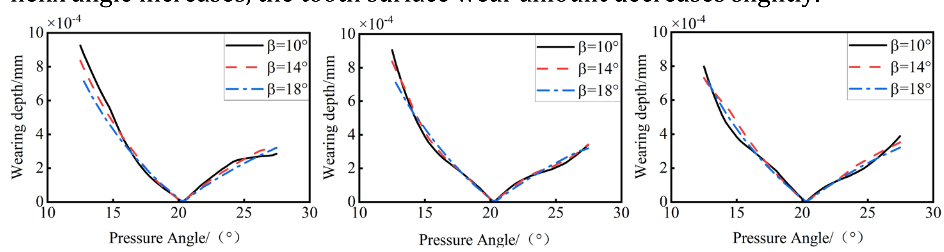

Figure 7. The wear amounts of the front, middle and rear end faces under different helix angles

Figure 8 shows the tooth surface wear amounts of the driving wheel when the face widths are 45mm, 55mm, and 65mm respectively. As the face width increases, the load per unit contact line and contact pressure decrease, leading to a significant reduction in the tooth surface wear amount.

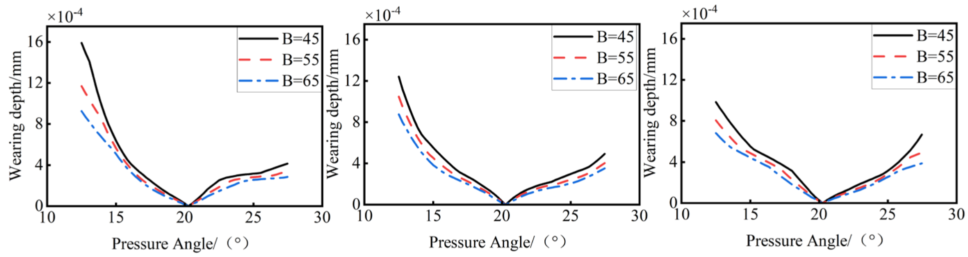

Figure 8. The wear amounts of the front, middle and rear end faces under different tooth widths

Taking a certain type of bevel gear used in a certain high-speed train as the object, the tooth surface wear amount calculation and related parameters analysis were conducted. The calculation results of the tooth surface wear amount of the driving and driven wheel surfaces showed that the wear amount at the root and tip of the teeth was relatively large, and the wear amount at the root was greater than that at the tip. The wear amount at the pitch circle tended to be zero. From the front to the rear of the gear's front surface, the wear amount of the driving wheel gradually decreased while that of the driven wheel gradually increased; the wear amount of the wide gear gradually became evenly distributed along the tooth width. The parameter analysis indicated that increasing the module, the tooth width, or reducing the torque could reduce the wear amount, while increasing the helix angle had no obvious effect on reducing the tooth surface wear.

References

[1] Wu S, Cheng H S. A sliding wear model for partial-EHL contacts[J]. Journal of Tri bology, 1991, 113(1):134-141.

[2] Wu S, Cheng H S. Sliding wear calculation in spur gears[J]. Journal of Tribology, 1993, 115(3):493-500.

[3] Hsu S M, Shen M C, Ruff A W. Wear prediction for metals[J]. Tribology Interna tional, 1997, 30(5):377-383.

[4] Flodin A, Andersson S. Simulation of mild wear in helical gears[J]. Wear, 2000, 241(2):123-128.

[5] Flodin A, Andersson S. A simplified model for wear prediction in helical gears[J]. Wear, 2001,249(3):285-292.

[6] Bajpai P, Kahraman A, Anderson N E. A surface wear prediction methodology for parallel-axis gear pairs[J]. Journal of Tribology, 2004, 126(3):597-605.

[7] Kahraman A, Bajpai P, Anderson N E. Influence of tooth profile deviations on hel ical gear wear[J]. Journal of Mechanical Design, 2005, 127(4):656-663.

[8] Hegadekatte V, Hilgert J, Kraft O, et al. Multi time scale simulations for wear pre dition in micro-gears[J]. Wear, 2010, 268(1):316-324.

[9] Ding H, Kahraman A. Interactions between nonlinear spur gear dynamics and surface wear. Journal of Sound & Vibration, 2007, 307(3–5):662-679

[10] Liu X, Yang Y, Zhang J. Investigation on coupling effects between surface wear and dynamics in a spur gear system. Tribology International, 2016, 1 01:383-394

[11] Osman T, Velex P. Static and dynamic simulations of mild abrasive wear in wide-faced solid spur and helical gears. Mechanism & Machine Theory, 2010, 45(6):911-924.